RESEARCH PAPER

Anti-cancer active nano carbon drug conjugate based on an Aryl Azide using the classical 'click' chemistry

Sujeet Kumar Thakur[1,2], Riya Ghosh[3,4], Prasenjit Guchhait[3*], Sambasivan Venkat Eswaran[2,5*]

[1]TERI School of Advanced Studies, (Plot No. 10, Vasant Kunj Institutional Area), New Delhi-110070, India
[2] BEMMS, 4C-1G, Foundation for Innovation and Technology Transfer, Indian Institute of Technology Delhi, Hauz Khas, New Delhi, Delhi 110016, India
[3]Regional Centre for Biotechnology (RCB), Under the Auspices of UNESCO-DBT, (NCR Biotech Science Cluster), 3rd Milestone, Faridabad-Gurgaon Expressway, Faridabad-121001, Haryana, India
[4]Manav Rachna International Institute of Research and Studies, Faridabad, India
[5]Ex: Head (Chemistry Department) and Dean (Academics), St Stephen's College, Delhi, 110007; Amity University, Noida, Uttar Pradesh-201313, India; Adjunct Prof. (Hony.), Deakin University, Australia; Teri Deakin Nano Biotechnology Research Centre, Gwal Pahari, TERI Gram, The Energy and Resources Institute, Gurgaon Faridabad Road, Gurgaon, Haryana 122 002, India

ABSTRACT

Objective(s): Nano Carbon Drug Conjugates (NCDCs) are created by attaching therapeutic agents to nanocarbon structures such as Fullerene (C_{60}), Single-Walled Carbon Nanotubes (SWCNT), Graphene Oxide (GO), and Reduced Graphene Oxide (rGO). These conjugated nanocarriers exhibit outstanding characteristics, including a high surface area, ease of functionalization, and the ability to penetrate biological barriers.

Materials and Methods: The conjugation of drugs to these nanocarriers enhances the solubility, stability, and bioavailability of the drugs, potentially overcoming the limitations of conventional drug delivery systems, such as cytotoxicity and side effects. The design of Nano Carbon Drug Conjugates (NCDCs) requires careful consideration of factors like the Drug-to-Nanocarbon Ratio (DNR), the choice of linker, and the selection of a targeting moiety to ensure selective accumulation in diseased tissues while minimizing off-target effects. NCDCs have broad applications in various medical fields, with a significant emphasis on cancer therapy (oncology), where they can deliver cytotoxic agents directly to tumor cells, thereby reducing systemic toxicity.

Results: This paper focuses on synthesis and characterizing a novel nanocarbon drug conjugate based on conventional 'click' chemistry, offering an improved approach for conjugating nanocarbons [(e.g. Fullerene C_{60})] with therapeutic agents. Additionally, it explores whether these conjugates could serve as theranostic agents.

Conclusions: The cytotoxicity of the newly prepared conjugate was evaluated using the MTT assay, and the cell survival rate was 87.68% at 10 µM and 79.73% at 20 µM, respectively, after 36 hours of treatment. Western blot analysis revealed significant expression of apoptosis markers, including Bax, Caspase 9, Cleaved Caspase 9, and Cytc, at 10 µM and 20 µM concentrations.

Keywords: *Anti-cancer activity; Classical 'Click' chemistry; Doxorubicin; Fullarazir; Nano Carbon Drug Conjugate.*

How to cite this article
Thakur SK, Ghosh R, Guchhait P, Eswaran SV. Anti-cancer active nano carbon drug conjugate based on an Aryl Azide using the classical 'click' chemistry. Nanomed J. 2025; 12: 1-. DOI: 10.22038/NMJ.2025.80781.1998

INTRODUCTION

NCDCs have emerged as a novel class of targeted therapeutic agents to improve the efficacy and safety of anticancer treatments, similar to antibody-drug conjugates (ADCs) and small-molecule drug conjugates (SMDCs). These NCDCs selectively deliver drugs, enhance solubility, and reduce side effects [1-3]. This precise delivery is achieved by exploiting the unique properties of nanocarbons, such as fullerenes, carbon nanotubes, and graphene, which can be functionalized with therapeutic molecules. One of the key advantages of NCDCs is their ability to target cancer cells without damaging healthy tissues, which is beneficial for treating cancer, HIV, and other infections [4-6].

Recent studies highlight the potential of nanocarbon materials and their conjugates in applications such as vaccines, drug carriers, enhanced therapeutics, and diagnostics [7-10]. The synthesis of nanocarbon materials and their conjugates has garnered significant attention across various scientific fields [11]. Nanotechnology is a multidimensional scientific discipline encompassing molecular engineering and nanomedicine, mimicking biological processes and leveraging nanoscale dimensions' unique properties (1-100 nm) [12-14]. The attachment of ligands, such as drugs, antibodies, proteins, and peptides, can enhance specificity and enable targeted control of disease [15, 16]. Conjugating

*Corresponding author(s) Email: sv.eswaran@gmail.com; prasenjit@rcb.res.in. Note. This manuscript was submitted on June 26, 2024;

nanocarbon materials with drug molecules has demonstrated potential in managing side effects in biological systems [17]. The conjugation of drugs and nanocarbons can be achieved using various approaches, such as through a 'click' reaction for bio-orthogonal interactions, which play a crucial role in many biological processes [18-19]. Functional groups like amines, carboxylic acids, and thiols facilitate favorable reaction rates in aqueous solutions in 'click' chemistry, making it highly recommended for studies on biocompatibility and bio-orthogonality [20]. Copper-catalyzed cycloaddition is the classical 'click' chemistry, while strain-promoted alkyne-azide coupling (SPAAC) is a copper-free variant. The inverse-demand Diels-Alder reaction (iEDDA) with tetrazine and trans-cyclooctene (TCO) enables instantaneous reactions with very high yields [21-22]. 'Click' chemistry is also widely used in nanoparticle modification, targeted drug delivery, imaging, and discovery [23-25].

Specific advantages of hybrid nanoparticle-conjugated drugs include enhanced stability, biocompatibility, improved permeability, the enhanced permeability and retention (EPR) effect, and precise targeting. These properties result in significantly better efficacy than conventional drugs [26].

In this paper, we report the preparation of a novel nanocarbon drug conjugate, where Fullerene (C60)-based nanocarbon "Fullarazirman" is used to derive a new nanocarbon material, "Fullarazir," following the loss of manganese in the form of Manganese Disulfide (MnS_2). Passing hydrogen disulfide (H_2S) gas through a methanolic solution of Fullarazirman introduces free carboxylic acid groups on the molecule, which are then utilized for further conjugation. The free carboxylated "Fullarazir" was subjected to esterification with 4-butyne-1-ol to generate an alkylated analog. In a separate step, Doxorubicin was used as the drug, along with a heterobifunctional cross-linker containing an azido group. Overnight incubation at room temperature initiates the classical 'click' reaction, which was used for conjugation to obtain the final product. This nanocarbon drug conjugate was characterized using advanced techniques such as MALDI-MS, UV-Visible, FT-IR, Zeta potential, and fluorescence spectroscopy. The biological activity was evaluated using the MTT assay with the 4T1 breast cancer cell line, and Western blot analysis was compared with Doxorubicin, revealing its anti-cancer activity.

These studies demonstrate the successful synthesis and characterization of the new nanocarbon drug conjugate using classical 'click' chemistry. The MTT assay and Western blot analysis results indicate promising anti-cancer activity of this novel conjugate.

MATERIALS AND METHODS

Fullerene C60 (greater than 99.9% purity) was purchased from Sigma Aldrich. All other chemicals used in this study were also obtained from Sigma Aldrich. The in-house nanocarbon “Fullarazirman,” one of the novel compounds prepared in our laboratory, was used to obtain carboxylic acid-decorated molecules after the loss of manganese upon passing H_2S gas through a methanolic solution of "Fullarazirman." An in-house heterobifunctional crosslinker (CXL) and Doxorubicin (used as the drug) were employed in the conjugation process. Characterization studies of the crosslinker (CXL) revealed the presence of a thermally reactive NHS group and a photoreactive azide group at either end [loc. cit]. These functional groups undergo a two-step reaction to form the Nano Carbon Drug Conjugate (NCDC). The protocol for preparation and the procedure followed for the preliminary characterization studies are described below.

Materials required for cross-linker- doxorubicin conjugate

Doxorubicin, in-house prepared crosslinker, sodium bicarbonate, methanol, dichloromethane (DCM), and phosphorus pentoxide (P_2O_5).

MALDI-MS studies

The prepared samples were mixed with the sinapinic acid matrix in a 1:1 and 1:5 ratio. The solution was vortexed and centrifuged for 2 minutes at 7000 rpm, then spotted onto the sample holder. The mass spectrum was recorded using a SCIEX TOF/TOF 5800 mass spectrometer. UV-Visible spectra were obtained from the Nano Carbon Drug Conjugate (NCDC) methanol solution using a Perkin Elmer Lambda 35 double-beam spectrophotometer and a Nanodrop spectrophotometer (GE Healthcare). Fourier Transform Infrared (FT-IR) spectroscopy was used for functional group identification, and the spectrum was recorded using NCDC's methanol solution. The particle size was determined using a methanol solution and a Zetasizer Nano ZS90 (0.3 nm - 5.0 microns diameter). Fluorescence spectroscopic studies confirmed the presence of NCDC, utilizing the Perkin Elmer Lambda 35 double-beam spectrophotometer for fluorescence spectroscopy.

Synthesis of cross-linker

Synthesis of 2-Azido-3-methoxybenzoic acid-2, 5-dioxo-pyrrolidin-1-yl ester

The new heterobifunctional crosslinker, 2-Azido-3-methoxybenzoic acid-2,5-dioxo-pyrrolidin-1-yl ester (135 mg), was synthesized from 2-Amino-3-methoxybenzoic acid (200 mg, 1.19 mmol). The acid was dissolved in 8 mL of concentrated hydrochloric acid and 2 mL of water, then cooled to 0°C. Sodium nitrate (140 mg, 1.2 mmol) was slowly added in a minimal amount of water to diazotize the solution. A solution of sodium azide (NaN_3, 120 mg, 2 mmol) and sodium acetate (3.36 g, 40 mmol) in a minimal amount of water was then added slowly to the diazotized solution, resulting in the formation of an off-white solid at the bottom [27].

2-Azido-3-methoxybenzoic acid-2, 5-dioxo-pyrrolidin-1-yl ester–Doxorubicin conjugates (Cross-linker –Doxorubicin conjugate)

Doxorubicin contains an amine-reactive group that displaces the NHS group in the crosslinker (CXL). The crosslinker also contains an azide group, which becomes reactive and undergoes a 'click' reaction, forming a conjugate with the triple bond.

Procedure

Synthesis of CXL-doxorubicin conjugate (Step-1)

Five milligrams of Doxorubicin were weighed into a round-bottom flask, and sodium bicarbonate solution was added dropwise using a dropper to obtain a basic solution of Doxorubicin. Three milligrams of the 2-Azido-3-methoxybenzoic acid-2, 5-dioxo-pyrrolidin-1-yl ester crosslinker (CXL) were mixed with 5 mL of dichloromethane (DCM) in a beaker. The prepared CXL solution was then added to the round-bottom flask, changing the color from orange to violet. The solution was evaporated using a rotary evaporator (rotavapor), indicating the reaction between the CXL and Doxorubicin. The mixture was stirred overnight using a magnetic stirrer under a nitrogen (N_2) atmosphere to maintain an inert environment. Following this, the mixture was vacuum-dried in a desiccator with P_2O_5 overnight. The Doxorubicin-crosslinker conjugate was obtained in powder form, weighed, and used for the subsequent step as shown in (SI-1).

Characterization data

Molecular ion peak: m/z (973.1814 - 27.9947 = 945.1867 + 1H = 946.1937 (Calculated); Observed Peak = 946.4580; Error percentage = 0.027). The MS/MS spectrum of the drug–CXL conjugates shows the most intense peaks at 207.1924, 326.2153, 397.0867, 527.1072, 550.3742, and 821.3133, indicating the presence of Doxorubicin. UV-Visible spectrum in methanol shows absorption peaks at 370 nm, 409 nm, 470 nm, 500 nm, 507 nm, 524 nm, and 540 nm. The IR spectrum (in methanol) shows the following peaks: 667.66, 905.90, 1082.08, 1168.26, 1435.52, 1541.70, 1642.79, 2011.41, 2339.97, 2367.31, 2519.77, 2601.02, 2863.97, 3049.79, and 3323.07, as shown in (SI-2, SI-3).

The above characterization data shows the successful synthesis of the cross-linker and Doxorubicin conjugation.

Synthesis of Nano-Carbon Drug Conjugate (NCDC)

Synthesis of S-Tri-(1-Aziridino-2,3-Dimethoxy-Benzene-5-Carboxylato-6-Carboxylic Acid)-H-Fullerene C60–Manganese (II) Tri-Adduct Complex ("Fullarazirman"): Thirty milligrams of 'azido meta-meconine' (I) were placed in a round-bottom flask along with 30 mg of Fullerene (C60) and 6 mL of ortho-dichlorobenzene. A few pumice stones were added, and the solution was stirred with a magnetic stir bar in an oil bath under a nitrogen atmosphere, heated to 170–175°C for 7 hours. After 2 hours, two additional portions of 'azido meta-meconine' (30 mg each) were added at 2-hour intervals. After cooling, excess methanol was added, causing the product to precipitate as a brown solid. This precipitate was filtered and dried overnight in a vacuum desiccator with phosphorus pentoxide. To the solid, 3–5 drops of water, 2–3 pellets of sodium hydroxide (NaOH), and 10 g of potassium permanganate solution were added, which resulted in a color change to purple. The reaction mixture was then heated in a water bath and stirred for 7 hours. After cooling to room temperature, sodium sulfite and concentrated hydrochloric acid were added repeatedly until the solution became colorless. Precipitation was carried out by adding excess methanol. The mixture was filtered, and the insoluble part was separated. The filtrate was subjected to distillation to obtain "Fullarazirman" as the final product.

Synthesis of Fullarazir

Two hundred milligrams of "Fullarazirman" were placed in a round-bottom flask with 50 mL of methanol to prepare a methanolic solution. Hydrogen disulfide (H_2S) gas was passed in excess through the solution, and a black solid precipitated at the bottom of the flask, as shown in the schematic in Figure 1.

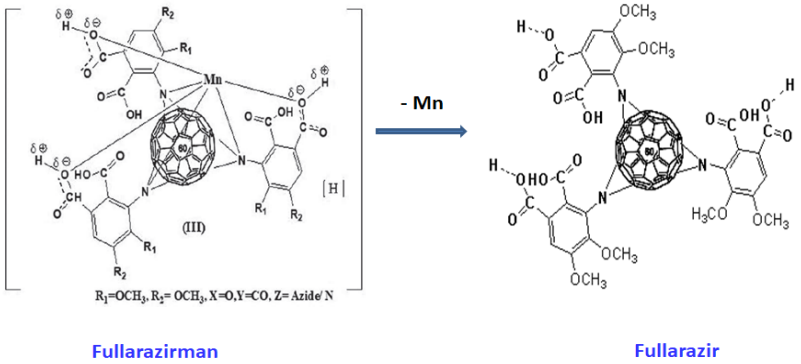

Fig. 1. Schematic of Fullarazirman to Fullarazir Conversion to make carboxylic acid free

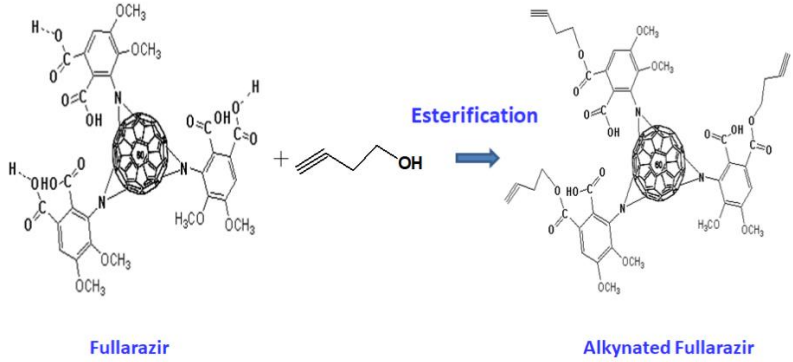

Fig. 2. Schematic of Alkynated Fullarazir

After obtaining the black solid, the solution was filtered and dried using a Büchi evaporator. "Fullarazirman" without Manganese, referred to as "Fullarazir," was obtained with a yield of 160 mg.

Synthesis of alkynated Fullarazir

Seventy-five milligrams of Fullarazir were placed in a round-bottom flask, and 11 mL of 4-butyne-1-ol was dissolved in 25 mL of dichloromethane (DCM) and 2 mL of diethyl ether. To this reaction mixture, 35 mg of dicyclohexylcarbodiimide (DCC) was added, and the solution was stirred overnight at room temperature. The color of the solution remained white, and the structural schematic is shown in Figure 2.

After overnight stirring, the mixture was filtered, yielding a colorless solution. This solution was then subjected to rotary evaporation (Büchi), and the desired product was obtained with a yield of 54 mg. The product was dried in a vacuum desiccator and further recrystallized from benzene.

UV-visible studies of alkynated fullarazir

Table 1 shows UV-visible data of the methanolic solutions of the starting material ("Fullarazirman") and Fullarazir after manganese removal. The data is compared to native fullerene, which shows peaks at 213 nm, 257 nm, and 229 nm, indicating no surface modification. However, for "Fullarazirman," Fullarazir, and alkylated Fullarazir (SI-4), shifts in the absorption bands are observed, indicating surface modification through the abovementioned methods.

This table shows a shift in the peaks of Fullarazir and alkylated Fullarazir (2-20 nm) when an electron-withdrawing group (alkyne) is attached to the carboxylic group present on the Fullarazir surface. This shift in the peaks indicates the successful synthesis of alkylated Fullarazir.

Table 1. UV visible Spectral data of Fullerene, "Fullarazirman", Fullarazir, and Alkynated

Sr. no	Fullerene (native in nm)	Fullarazirman (Starting Material in nm)	Fullarazir (nm)	Alkynated Fullarazir (nm)
1	213	369	210	212
2	257	372	220	215
3	229	374	235	260
4		377	245	272
5		382	290	
6		384		

FT-IR studies of Alkynated Fullarazir

The FT-IR Spectrum in Table 2 was obtained using the methanolic solution of "Fullazirman," "Fullarazir," and alkylated Fullarazir.

FT-IR studies of "Fullarazirman" show peaks at 1072 cm^{-1}, 1153 cm^{-1}, 1432 cm^{-1}, 1650 cm^{-1}, 1704 cm^{-1}, 2924 cm^{-1}, and 3406 cm^{-1} (loc. cit.). After the removal of manganese, the spectra of "Fullarazirman" and Fullarazir are similar, with peaks observed at 1077 cm^{-1}, 1178 cm^{-1}, 1436 cm^{-1}, 1669 cm^{-1}, 1727 cm^{-1}, 2861 cm^{-1}, 3041 cm^{-1}, and 3781 cm^{-1}, indicating the presence of carboxylic acid and hydrogen bonding with the OH group. After manganese removal, Fullarazir was used for alkyne attachment via esterification. The FT-IR spectral data of the resulting product show peaks at 1022 cm^{-1}, 1143 cm^{-1}, 1211 cm^{-1}, 1509 cm^{-1}, 1667 cm^{-1}, 2041 cm^{-1}, 2051 cm^{-1}, 2161 cm^{-1}, 2838 cm^{-1}, 2952 cm^{-1}, and 3311 cm^{-1}, confirming the presence of a terminal alkyne and other substituents for further study (SI-5 to SI-7).

Synthesis of fullarazir-doxorubicin conjugate

Ten milligrams of alkylated Fullarazir and 17 milligrams of the Doxorubicin-methoxy crosslinker containing an azide group were added to 20 mL of a solution containing dimethylformamide (DMF) and water in a 4:1 ratio. This mixture added 1.24 mg of sodium ascorbate and 1 mg of copper sulfate.

The reaction mixture was stirred with a magnetic stir bar at room temperature overnight. After stirring, the mixture was filtered and diluted with water, precipitating a solid at the bottom of the flask. The solid was filtered, and the desired product (25 mg) was obtained. This product was named "Fullarazir-Doxorubicin conjugate" and represents the Nano-Carbon Drug Conjugate (NCDC), as shown in Figure 3.

Anti-cancer test

The 4T1 breast cancer cell line was treated with either NCDC or Doxorubicin (Doxo) at concentrations of 10 or 20 µM for 36 hours. Cytotoxicity was assessed using the MTT assay. The pro-apoptotic markers, including Bax, cleaved caspase 9, and cytochrome C, were measured by Western blotting.

Table 2. FT-IR spectral data for "Fullarazirman", Fullarazir, and Alkynated Fullarazir

Sr. No	Fullarazirman in (cm^{-1})	Fullarazir (cm^{-1})	Alkynated Fullarazir (cm^{-1})
1	1072	1077	1022
	1153	1178	1143
	1432	1436	1211
	1650	1669	1509
	1704	1727	1667
	2924	2861	2041
	3406	3041	2051
		3781	2161
			2838
			2952
			3311

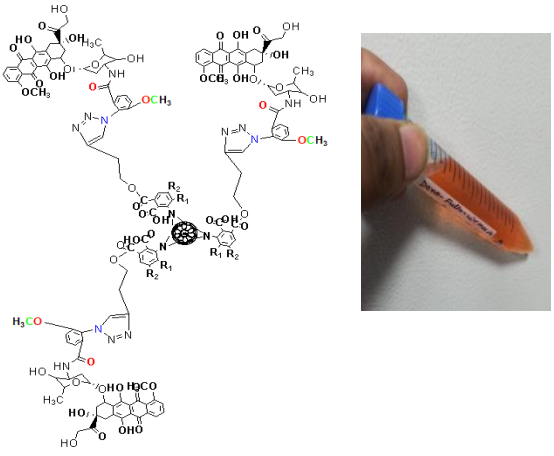

Fig. 3. Proposed structure and image of Fullarazir-Doxorubicin Conjugate (NCDC).

RESULTS AND DISCUSSION

Characterization of NCDC

Modern characterization techniques, such as MALDI-MS, UV-visible, FT-IR, UV-fluorescence, Zeta, etc., have been used to characterize the Fullarazir-Doxorubicin conjugate.

MALDI-MS studies of the NCDC

The mass spectrum of NCDC is recorded in methanolic solution and obtained at m/z 1046.54, 1296.66, 1369.80, 1619.82, 2093.09, 2465.18, and 3147.47, as shown in Figure 4.

The proposed molecular Formula – $C_{207}H_{145}N_{15}O_{57}$; Molecular peak m/z (787.2574*3= 2361.7722 + 1386.8323= 3747.6145 (Calculated) Observed Peak = 3748.6145- (3*$COCH_2OH$ - 177.0399) - (3*OH- 50.9994) - (3*H_2O-54.0459) – (6*OCH_3- 186.1104)- (3*CO_2- 131.9694) = 3747.6145 – 600.1650 = 3147.4495 = 3147.4415 ~ 3147.47 (Observed) Error = 0.0009 %.

The other peaks at m/z 2093. 09 are attributed to C90 H26 N3 O15 =1387.8323 + C39 H39 N4 O14 = 787.2574)-(2*OCH3- 62.0368)-(H2O-18.0153) - (1H-1.008) = 2094.0296 (error -0.044%), which confirms the two fragments of this conjugate.

The peak was obtained at 1296. 66 reflects for the fragment of (m/z $C_{90}H_{26}N_3O_{15}$ =1387. 8323- (2* OCH_3- 62.0368) - (CO- 28.0101) =1297.7854- (1H-1.008) = 1296.7846 (calculated), the Error percent is 0.009 %.

The highly intense peak obtained at 1046.54 is attributed to the loss of 249.9823 (3 * N_2- 84.0183)-(3*CO_2- 131.9694)—(2*OH—33.9996) from the m/z ($C_{90}H_{26}N_3O_{15}$ = 1387.8323).

The above mass spectrum analysis confirms the different fragmentation patterns resulting from the loss of (N2, CO, COO, OH, H2O) and the successful conjugation of nanocarbon material and doxorubicin through classical 'click' chemistry [28].

UV-visible studies of NCDC

UV-Visible studies show peaks at 209 nm, 219 nm, 230 nm, 249 nm, 290 nm, 359 nm, 485 nm, 529 nm, and 560 nm, as shown in Figure 5.

The peaks at 209 nm, 219 nm, 230 nm, and 290 nm are attributed to the starting material, "Fullarazirman," and the used linker. In contrast, the peaks at higher wavelengths, such as 359 nm, 485 nm, 529 nm, and 560 nm, confirm the successful conjugation of Doxorubicin with Fullarazir [29].

FT-IR studies of NCDC

FT-IR studies are valuable for functional group identification, with the spectrum range used being 400 to 4000 cm^{-1}. Previous studies on Doxorubicin show peaks at 1065 cm^{-1}, 1338 cm^{-1}, 1638 cm^{-1}, and 3410 cm^{-1}, corresponding to the involvement of various functional groups [30].

The FT-IR spectrum of the NCDC (shown in Figure 6) shows peaks at 1020 cm^{-1}, 1122 cm^{-1}, 1414 cm^{-1}, 1666 cm^{-1} (-COOH), 2546 cm^{-1} (C=C conjugation), 2825 cm^{-1}, 2949 cm^{-1} (aliphatic CH and CH_2 groups), and 3296 cm^{-1} (OH with hydrogen bonding). These results further confirm the successful synthesis of the Fullarazir-Doxorubicin conjugate using the in-house cross-linker.

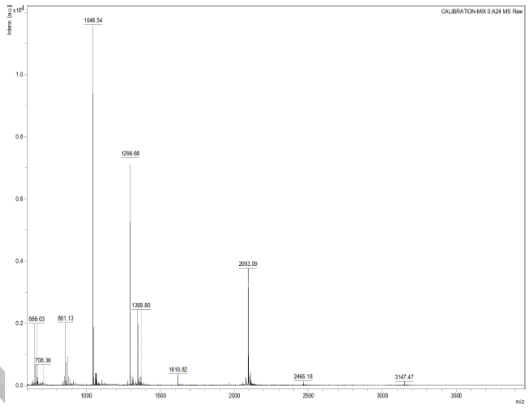

Fig. 4. MALDI-MS spectrum of NCDC

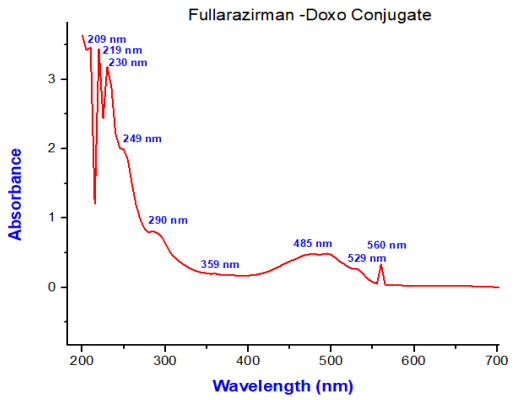

Fig. 5. UV-Visible spectrum of NCDC

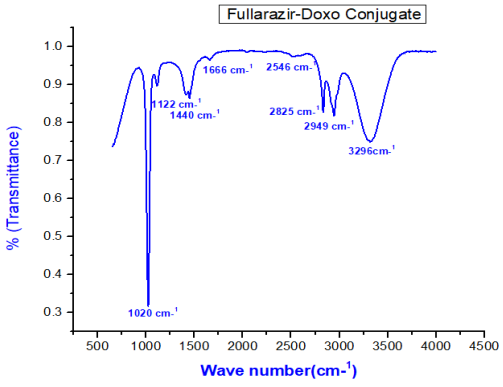

Fig. 6. FT-IR spectrum of NCDC

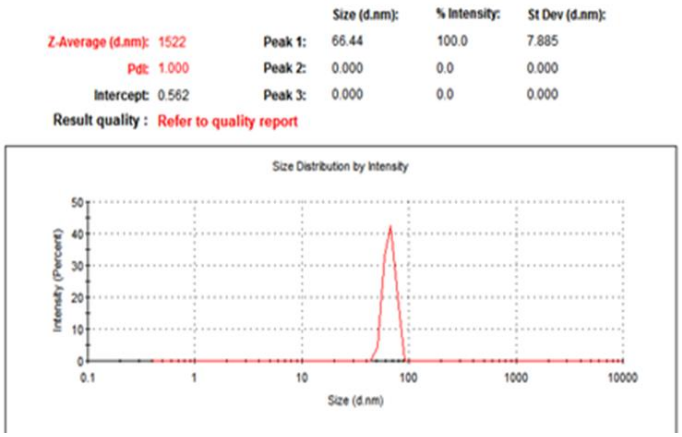

Fig. 7. Zeta size spectrum of NCDC

Zeta size studies of NCDC

General physicochemical properties, such as delivery, encapsulation, loading efficiency, morphology, biodegradation, particle size, and charge [31], play a critical role in applied biology. Nanoparticles in the 10-500 nm range are widely reported to benefit from the tumor site-enhanced permeability and retention (EPR) effect [32].

The zeta size spectrum of the NCDC shows two peaks, indicating the presence of two types of particles, with a polydispersity index of 1.00, as shown in Figure 7.

One peak corresponds to a size of 64.44 nm, indicating the attachment of Doxorubicin, which is different from the starting material "Fullarazirman" (58.9 nm). This further confirms the conjugation of the nanocarbon material with the drug molecule [33, 34].

Fluorescence studies of NCDC

The three-dimensional structure of the molecules was analyzed using fluorescence spectroscopy, with the spectrum spanning the range of 250 nm to 800 nm, as shown in Figure 8.

The UV-fluorescence spectrum shows a peak at 249 nm, along with several other lower-intensity peaks observed at 214.8 nm, 307.0 nm, 441.6 nm, 704.6 nm, 727.0 nm, 746.6 nm, and 780.6 nm. These peaks, which may result from the conjugation of Fullarazir with the Doxorubicin conjugate, confirm the successful conjugation and formation of the NCDC, as shown in (SI-8) [35].

Biological activity

In the MTT assay (Figure 9), the concentration of the new Fullarazir-Doxorubicin conjugate (NCDC) [36] was tested to assess its anti-cancer activity. The MTT assay results show that the survival rate of 4T1 cells is approximately 87.68% at 10 µM and 79.73% at 20 µM after 36 hours of treatment, demonstrating its potential for further studies.

MTT studies of NCDC suggest that it could improve biocompatibility and stability in physiological buffers. The use of fullerene-based nanomaterials plays a critical role in targeted, pH-responsive drug delivery and represents a promising new modality for cancer therapy [37].

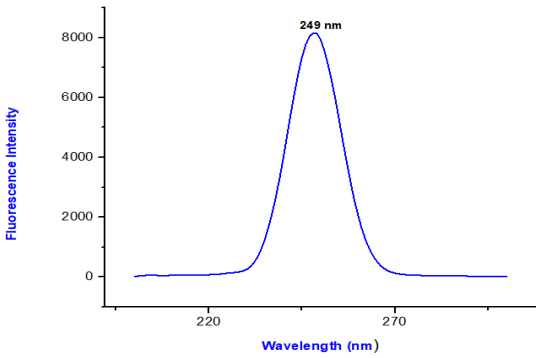

Fig. 8. Fluorescence spectrum of Fullarazir-Doxorubicin conjugate

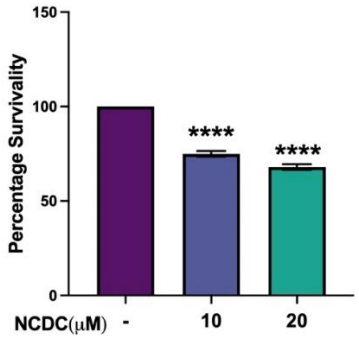

Fig. 9. MTT assay of Fullarazir -Doxorubicin conjugate (NCDC) shows the percentage survival of the 4T1 cell is approximately 87.68% at 10 µM and 79.73% at 20 µM concentration after 36-hour treatment

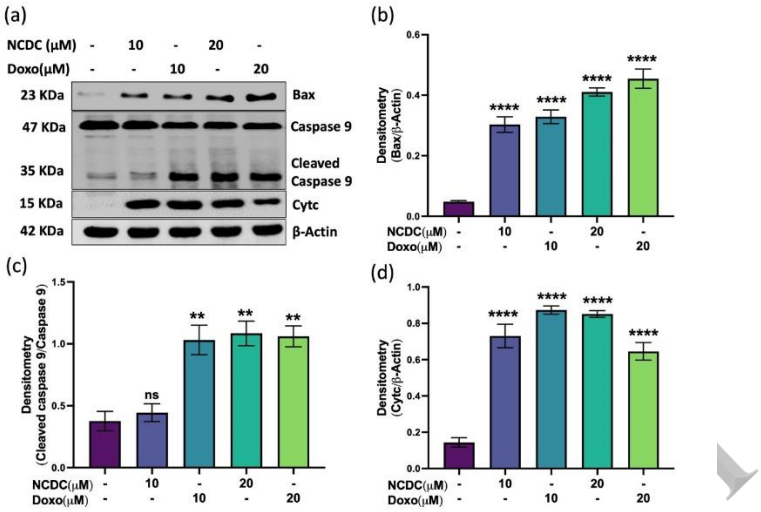

Fig. 10. Immunoblot of pro-apoptotic molecules showing efficient apoptosis-inducing ability in 4T1 breast cancer cell line treated with NCDC (Fullarazir Doxorubicin conjugate) and Doxorubicin with 10μM and 20μM conc. Doxorubicin was used as a positive control.

NCDC induces the expression of apoptosis-related molecules in 4T1 cells. In these experiments, the 4T1 breast cancer cell line was treated with either Doxorubicin or the titled complex (10 or 20 μM) for 36 hours, as shown in Figure 10.

The pro-apoptotic markers were measured, including Bax, Caspase 9, cleaved Caspase 9, and Cytochrome C (Cytc). The density of the cleaved band (35 kDa) of Caspase 9 showed increased cell death in the presence of NCDC treatment. Additionally, the apoptosis marker Bax was also elevated in the NCDC-treated group. β-Actin was used as the loading control.

CONCLUSION

A new nanocarbon drug conjugate has been developed and characterized spectroscopically. "Fullarazirman," synthesized earlier, was converted into Fullarazir by removing manganese through the passage of H_2S. Fullarazir was then esterified with 4-butyne-1-ol/DCC. Meanwhile, the well-known anti-cancer drug Doxorubicin was transformed into its corresponding amine, which was subsequently used to form an adduct with our novel aryl azido NHS crosslinker. These two newly synthesized components were subjected to 'click' chemistry, binding them through the formation of regiospecific 1,4-disubstituted-1,2,3-triazoles. This deep red nanocarbon drug conjugate was characterized using UV, FTIR, fluorescence spectroscopy, and zeta potential analysis. Mass spectral studies also supported the formation of the conjugate. The MTT assay of the new conjugate revealed cell survival rates of 87.68% at 10 μM and 79.73% at 20 μM. Furthermore, Western blot analysis showed upregulation of pro-apoptotic markers in the 4T1 breast cancer cell line at 10 μM and 20 μM concentrations. This newly developed conjugate is expected to benefit anti-cancer drug delivery systems.

ACKNOWLEDGEMENTS

The authors thank the Executive Director, Regional Centre for Biotechnology (RCB), Faridabad, Haryana, India, for research facilities. They also thank Mr. Vijay Kumar Jha (RCB, Faridabad) for FT-IR studies and Zeta potential measurement. Finally, they thank Mr. Manurbhav Arya (Ph.D. Scholar, TERI-SAS & Deakin University) for helping prepare the manuscript.

CONFLICT OF INTERESTS

There are no competing interests to disclose.

FUNDING

No funding was used for this Manuscript.

DATA AVAILABILITY

The data used to support the findings of this study have been deposited in the figshare repository 10.6084/m9.figshare.29447657”

REFERENCES

1. Sheingold BH, Hahn JA. The history of healthcare quality: the first 100 years 1860–1960. Intern J Appl Nonlinear Sci. 2014; 1:18–22.
2. Liebler D, Guengerich F. Elucidating mechanisms of drug-induced toxicity. Nat Rev Drug Discov. 2005; 4**:** 410–420.

3. Dubey D, Dhiman S, Koner AL. Review of Carbon Dot-Based Drug Conjugates for Cancer Therapy. ACS Applied Nano Materials. 2023; 6 (6): 4078-4096.
4. De Jong WH, Borm PJ. Drug delivery and nanoparticles: applications and hazards. Int J Nanomedicine. 2008; 3(2): 133-149.
5. Tiwari G, Tiwari R, Srivastava B, Bhati L, Pandey S, Pandey P, Bannerjee SK. Drug Delivery Systems: An Updated Review. Intern J Pharmaceutical Investi. 2012; 2: 1-10.
6. Emerich DF, Thanos CT. Targeted nanoparticle-based drug delivery and diagnosis. J Drug Target. 2007; 15 (3): 163-183.
7. Lu L, Duong VT, O Shalash AO, Skwarczynski M, Toth I. Chemical Conjugation Strategies for the Development of Protein-Based Subunit Nanovaccines. Vaccines. 2021; 9 (563):1-24.
8. Yi G, Son J, Yoo J, Park C, Koo H. Application of click chemistry in nanoparticle modification and its targeted delivery. Biomater Res. 2018; 22(13): 1-8.
9. Xie J, Lee S, Chen X. Nanoparticle-based theranostic agents. Adv Drug Deliv Rev. 2010; 62:1064–1079.
10. Lee DE, Koo H, Sun IC, Ryu JH, Kim K, Kwon IC. Multifunctional nanoparticles for multimodal imaging and theragnosis. Chem Soc Rev. 2012; 41: 2656–2672.
11. Bhattacharyya D, Singh S. Nanotechnology, big things from a tiny world: a review. Int. J. u- and e-Serv, Sci. Technol. 2009; 2(3): 29–38.
12. Emerich DF, Thanos C. The pinpoint promise of nanoparticle-based drug delivery and molecular diagnosis. Biomol Eng. 2006; 23:171–184.
13. Singh R, Lillard Jr JW. Nanoparticle-based targeted drug delivery. Exp Mol Pathol. 2009; 86: 215–223.
14. Biswas AK, Islam MR, Choudhary ZS, Mostafa A, Kadir MF. Nanotechnology based approaches in cancer therapeutics. Adv. Nat. Sci. Nanosci. Nanotechnol. 2014; 5(043001): 1-12.
15. Byrne JD, Betancourt T, Brannon-Peppas L. Active targeting schemes for nanoparticle systems in cancer therapeutics. Adv Drug Deliv Rev. 2008; 60: 1615–26.
16. Torchilin V. Tumor delivery of macromolecular drugs based on the EPR effect. Adv Drug Deliv Rev. 2011; 63: 131–5.
17. Odiba A, Ukegbu C, Anunobi O, Chukwunonyelum E, Esemonu J. Making drugs safer: improving dug delivery and redicing the side effect of drug on the human biochemical system. Nanotech Rev. 2016; 5(2): 183-194.
18. Bertozzi CR. A decade of bioorthogonal chemistry. Acc Chem Res. 2011; 44:651–53.
19. Kolb HC, Finn MG, Sharpless KB. Click chemistry: diverse chemical function from a few good reactions. Angew Chem Int Ed. 2001; 40: 2004–2021.
20. Yoon HY, Koo H, Kim K, Kwon IC. Molecular imaging based on metabolic glycoengineering and bioorthogonal click chemistry. Biomaterials. 2017;132: 28–36.
21. Jewett JC, Bertozzi CR. Cu-free click cycloaddition reactions in chemical biology. Chem Soc Rev. 2010; 39: 1272–1279.
22. Devaraj NK, Weissleder R. Biomedical applications of tetrazine cycloadditions. Acc Chem Res. 2011; 44: 816–827.
23. Majumder N. Click chemistry in nano drug delivery system and its applications in biology. IJRPC. 2015; 5: 95–105.
24. Colombo M, Sommaruga S, Mazzucchelli S, Polito L, Verderio P, Galeffi P, Corsi F, Tortora P, Prosperi D. Site-specific conjugation of ScFvs antibodies to nanoparticles by bioorthogonal strain-promoted alkyne–Nitrone cycloaddition. Angew Chem Int Ed. 2012; 51: 496–499.
25. Liu R, Zhao J, Han G, Zhao T, Zhang R, Liu B, Liu Z, Zhang C, Yang L, Zhang Z. Click-functionalized SERS Nanoprobes with improved labeling efficiency and capability for cancer cell imaging. ACS Appl Mater Interfaces. 2017; 9: 38222–38229.
26. Yao Y, Zhou Y, Liu L, Xu Y, Chen Q, Wang Y, Wu S, Deng Y, Zhang J, Shao A. Nanoparticle-Based Drug Delivery in Cancer Therapy and Its Role in Overcoming Drug Resistance. Front Mol Biosci. 2020; 7(193): 1-14.
27. Wang X, Hui R, Chen Y, Wang W, Chen Y, Gong X, Jin J. Discovery of Novel Doxorubicin Metabolites in MCF7 Doxorubicin-Resistant Cells. Front. Pharmacol. 2019; 1434: 1-11.
28. Chu H, Unnikrishnan B, Anand A, Mao J, Huang C. Nanoparticle-based laser desorption/ionization mass spectrometric analysis of drugs and metabolites, Journal of Food and Drug Analysis. 2018; 26(4): 1215-1228.
29. Bandak S, Ramu A, Barenholz Y, Gabizon A. Reduced UV-induced degradation of doxorubicin encapsulated in polyethyleneglycol-coated liposomes. Pharm Res. 1999; 16(6): 841-846.
30. Victor SP, Paul W, Jayabalana M, Sharma CP. Supramolecular hydroxyapatite complexes as theranostic near-infrared luminescent drug carriers. Cryst Eng Comm, 2014; 16: 9033–9042.
31. Juan A, Cimas FJ, Bravo I, Pandiella A, Alberto Ocaña A, Alonso-Moreno C. An Overview of Antibody Conjugated Polymeric Nanoparticles for Breast Cancer Therapy. Pharmaceutics. 2020; 12(802): 1-20.
32. Bawa R. FDA and Nanotech: Baby Steps Lead to Regulatory Uncertainty. In Bio-Nanotechnology, Blackwell Publishing Ltd.: Oxford, UK, 2013, 720–732.
33. Nakamura Y, Mochida A, Choyke PL, Kobayashi H. Nanodrug Delivery: Is the Enhanced Permeability and Retention Effect Sufficient for Curing Cancer?. Bioconjugate Chem.2016; 27: 2225–2238.
34. Ghassami E, Varshosaz J, Somayeh Taymouri S. Redox Sensitive Polysaccharide Based Nanoparticles for Improved Cancer Treatment: A Comprehensive Review. Current Pharmaceutical Design. 2018; 24: 3303-3319.
35. Behera SK, Mohanty ME, Mohapatra MA. Fluorescence Study of the Interaction of Anticancer Drug Molecule Doxorubicin Hydrochloride in Pluronic P123 and F127 Micelles. J Fluorescence. 2021; 31: 17–27.
36. Ye L, Kollie L, Liu X, Guo W, Ying Y, Zhu J, Yang S, Yu M. Antitumor Activity and Potential Mechanism of Novel

Fullerene Derivative Nanoparticles. Molecules. 2021; 26(11): 3252.
37. Tang L, Li J, Pan T, Yin Y, Mei Y, Xiao Q, Wang R, Yan Z, Wang W. Versatile carbon nanoplatforms for cancer treatment and diagnosis: strategies, applications and future perspectives. Theranostics. 2022; 12(5): 2290-2321.